International Journal of Engineering, Mathematical and Physical Sciences
ISSN: 2517-9934
Vol:8, No:3, 2014

Motion Planning and Posture Control of the General 3-Trailer System

K. Raghuwaiya, B. Sharma, J. Vanualailai

***Abstract*—**This paper presents a set of artificial potential field functions that improves upon, in general, the motion planning and posture control, with theoretically guaranteed point and posture stabilities, convergence and collision avoidance properties of the *general*3-trailer system in *a priori* known environment. We basically design and inject two new concepts; *ghost walls* and the *distance optimization technique* (DOT) to strengthen point and posture stabilities, in the sense of Lyapunov, of our dynamical model. This new combination of techniques emerges as a convenient mechanism for obtaining feasible orientations at the target positions with an overall reduction in the complexity of the navigation laws. Simulations are provided to demonstrate the effectiveness of the controls laws.

***Keywords*—**Artificial potential fields, 3-trailer systems, motion planning, posture.

I. Introduction

MOTION planning for tractor-trailer mobile robots is currently one of the most active areas of mobile robots technologies and has attracted the attention of many scholars in the field of robotics and control engineering. Following the appearance of various new methods and new technologies, researchers to date have more in-sight into the motion planning problem.

The nonholonomic motion planning problem involves finding a feasible path from some initial configuration to some desired final configuration for a system with nonholonomic velocity constraints. These nonintegrable constraints arise from the condition of non-slippage on the wheels in rolling contact with another rigid body. Some examples of these types of nonholonomic systems include mobile robots, tractor-trailer vehicles and mobile manipulators. A wide range of problems in various robotic applications have been solved by utilizing the artificial potential field method. Its major advantages include easier analytic representation of system singularities and inequalities, its simplicity and processing speed. The underlying principle of this method is to attach attractive fields to the target and repulsive fields to the obstacles. The robot's workspace is then filled with positive and negative fields, in which the robot is attracted to its designated target and repulsed away from the obstacles. The pioneer work on motion planning and control of robots via the artificial potential fields was done by Khatib in [1].

Tractor-trailer systems constitute a generalization of the mobile robots. They are basically composed of a mobile robot, and several trailers pulled by the mobile robot, which satisfy nonholonomic restrictions as well. Tractor trailer mobile robots have great applications in labor intensive work or in areas which pose a high risks to human health. These articulated robot systems are found in a variety of places, such as airports, factories, railway stations, nuclear power plants, mines, in multiple-trailer trucks as they increase transportation efficiency. Researchers are currently designing various control algorithms for motion planning of these multi-body vehicles that are capable of performing a wide range of tasks in various environments.

Many researchers have studied tractor-trailer systems with on axle hitching, but only a few have focused on the off-axle hitched trailer systems due to its kinematic structure which is highly complicated. As such, analysis and controller design becomes difficult, especially with rear wheel driven prime movers. In [2], the authors used a front wheel drive tractor to derive the kinematic model for the general n-trailer to solve the nonholonomic motion planning problem. In [3], Bolzernet al. proposed control laws for the off-axle hitched trailer system based on linearization of a virtual on-axle vehicle which shares some properties with the actual one. In [4], Lee et al. presented experimental data for the design and control of passive multiple trailer systems, both off and on-axle. Motion planning and collision avoidance schemes were considered by minimizing the trajectory tracking error with the reference trajectory implying the trajectory of the towing vehicle. In [5]-[9], the authors considered motion planning and posture control and formations types of the standard and general 1-trailer robots where point to point motion were controlled using a Lyapunov based control scheme. Ghost walls and the distance optimization technique (DOT) were utilized to orchestrate "near perfect" final orientations of every solid body of the articulated robot, inside a designated parking bay.

This paper makes use of Lyapunov techniques as a tool for themotion planning of tractor-trailer robots. Specifically, theauthors deal with the general 3-trailer system. Themulti-body robot navigates its way towards the target in aconstrained workspace populated with fixed obstacles. Here, thewalls of the bounded workspace and the static obstacles aretreated as ghost obstacles. To avoid these obstacles, we utilize Khatib's collision avoidance scheme to propose potential fields tosafely traverse in the workspace towards the

K. Raghuwaiya is with the School of Computing, Information and Mathematical Sciences at the University of the South Pacific, Fiji Islands (phone: +679 3232253; fax: +679 3231527; e-mail: raghuwaiya_k, singh_sb@ @usp.ac.fj).

B. Sharma is with the Faculty of Science, Technology and Engineering at the University of the South Pacific, Fiji Islands (phone: +679 3232069; fax: +679 3231527; e-mail: sharma_b@ @usp.ac.fj).

J. Vanualailai is with the Research Office at the University of the South Pacific, Fiji Islands (phone: +679 3232277; fax: +679 3231527; e-mail: vanualailai@usp.ac.fj).

target position andattain the desired final posture.

The paper is organized as follows. In Section II, the vehicle modelis defined. In Sections III, IV and V, motion planning is carried out. Theconstruction of stabilizing control laws is presented in SectionVI, while Section VII contains some simulation results. The paperends with some concluding remarks in Section VIII.

II. Vehicle Model

Two different trailer systems can be distinguished from literature; *standard* and the *general* trailer systems, grouped into two different categories based upon their different hooking schemes. Basically, these systems consist of a tractor towing an arbitrary number of trailers, which mostly are passive in order to reduce the costs ofimplementation. The authors will consider a rear wheel drivencar-like vehicle, and an off-axle (general system) hitched two-wheeled passive trailer, in Euclidian plane. The tractor robot utilized herein basicallyperforms motions similar to that of a car-like robot, with front-wheel steering and decrees the path of the attached trailer.

In this research, the *general*3-trailer system embodies a car-like tractor robot and three off-axle hitched two-wheeled passive trailers. That is, the trailer is not attached exactly to the midpoint of the rear axle of the tractor robot but here the coupling joint is located beyond the center point of the rear axle i.e. at a positive distance $d_i > 0$ (see Fig. 1}). Essentially, a kingpin joins the two solid bodies with $d_i > 0$ and L_i^G for $i = 0,...,3$, as positive lengths, from the midpoint of the rear axles of the two vehicles.

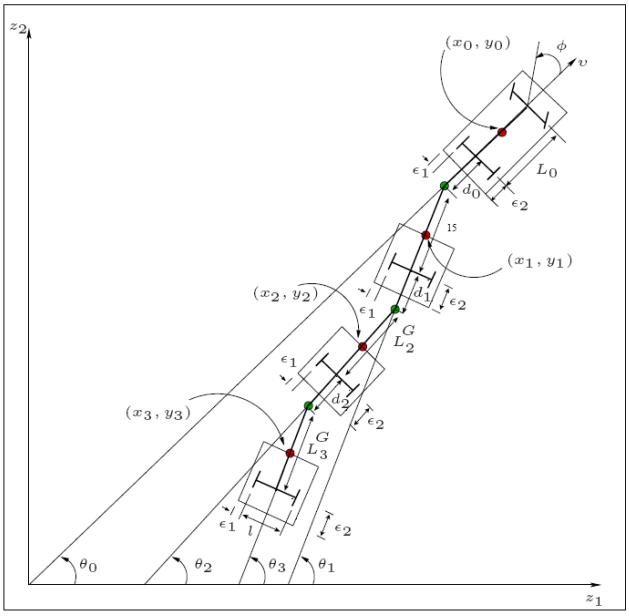

Fig. 1 Kinematic model of the general 3-trailer robot

With reference to Fig. 1, (x_i, y_i) represents the Cartesian coordinates and gives the reference point of the *i*th solid body of the articulated robot while θ_i gives its orientation with respect to the z_1 axis. Also, L_0 is the distance between the two axles of the tractor robot, and *l* is the length of each axle. The connections between any two bodies give rise to the following holonomic constraints on this system:

$$x_i = x_0 - \left(\frac{L_0 + 2d_0}{2}\right)\cos\theta_0 - \sum_{j=1}^{i-1}\left(L_j^G + d_j\right)\cos\theta_j - \left(\frac{L_i^G + d_i}{2}\right)\cos\theta_i$$

$$y_i = y_0 - \left(\frac{L_0 + 2d_0}{2}\right)\sin\theta_0 - \sum_{j=1}^{i-1}\left(L_j^G + d_j\right)\sin\theta_j - \left(\frac{L_i^G + d_i}{2}\right)\sin\theta_i$$

for $i = 0,...,3$. We define $d_i := \varepsilon_1 + a_i$ where a_i is a small offset for the *i*th vehicle (see Fig. 2). These constraints will reduce the dimensionof the configuration space, since the position (x_i, y_i) can be expressed completely in terms of (x_o, y_0, θ_i) for $i = 0,...,3$.

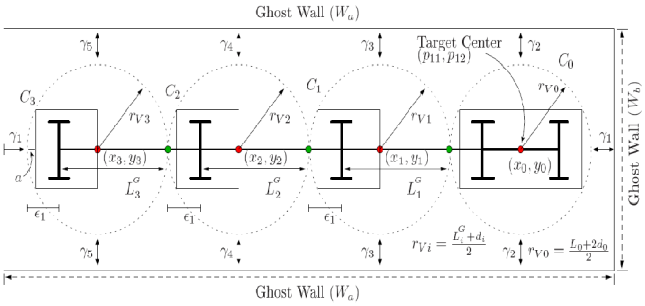

Fig. 2 Schematic diagram of a general 3-trailer system and the *ghost walls*

If we let *m* be the mass of the full robot, *F* the force along the axis of the tractor robot, Γ the torque about a vertical axis at (x_o, y_0) and *I* the moment of inertia of the tractor robot, then the dynamic model of a general 3-trailersystem extended from [5] is given in (1).

The selection of the reference points is due to the simplicity in the construction of the potential field functions. It is important to note that when $d_i = 0$, the kinodynamical model for the off-axle hitching is exactly the same as that of the 0n-axle hitching, provided we define $L_i^G = L_i^S$, where L_i^S is the corresponding length for the standard trailer system.

A. Minimizing C-Space

To ensure that the entire vehicle safely steers pass an obstacle,the planar vehicle can be represented as a simpler fixed-shapedobject, such as a circle, a polygon or a convexHull [10]. This representation is facilitated with theinherent view of minimizing the obstacle space in the workspace.

$$
\left.\begin{aligned}
\dot{x}_0 &= v\cos\theta_0 - \tfrac{L}{2}\omega\sin\theta_0,\\
\dot{y}_0 &= v\sin\theta_0 + \tfrac{L}{2}\omega\cos\theta_0,\\
\dot{\theta}_0 &= \frac{v}{L_0}\tan\phi := \omega,\\
\dot{\theta}_i &= \frac{1}{L_i^G}\left\{\sin\left(\theta_{i-1}-\theta_i\right)\left[\prod_{j=1}^{i-1}\cos\left(\theta_{j-1}-\theta_j\right)\right]\right.\\
&\quad +\left\lfloor\tfrac{i}{2}\right\rfloor(-1)^{i+1}\sin\left(\theta_0-\theta_1\right)\left[\prod_{j=2}^{i}\frac{d_{j-1}}{L_{j-1}^G}\cos\left(\theta_{j-1}-\theta_j\right)\right]\\
&\quad +\left\lfloor\tfrac{i}{3}\right\rfloor\sin\left(\theta_1-\theta_2\right)\left[\frac{d_1}{L_1^G}\sin\left(\theta_2-\theta_3\right)\sin\left(\theta_0-\theta_1\right)\right]\\
&\quad \left.-\left\lfloor\tfrac{i}{3}\right\rfloor\sin\left(\theta_1-\theta_2\right)\left[\frac{d_2}{L_2^G}\cos\left(\theta_2-\theta_3\right)\cos\left(\theta_0-\theta_1\right)\right]\right\}v\\
&\quad +\frac{d_0}{L_i^G}\left\{(-1)^i\cos\left(\theta_0-\theta_1\right)\left[\prod_{j=1}^{i-1}\frac{d_j}{L_j^G}\cos\left(\theta_j-\theta_{j+1}\right)\right]\right.\\
&\quad +\left\lfloor\tfrac{i}{2}\right\rfloor(-1)^i\left[\prod_{j=0}^{1}\sin\left(\theta_j-\theta_{j+1}\right)\right]\left[\prod_{k=3}^{i}\frac{d_{k-1}}{L_{k-1}^G}\cos\left(\theta_{k-1}-\theta_k\right)\right]\\
&\quad +\left\lfloor\tfrac{i}{3}\right\rfloor\sin\left(\theta_2-\theta_3\right)\left[\cos\left(\theta_1-\theta_2\right)\sin\left(\theta_0-\theta_1\right)\right]\\
&\quad \left.-\left\lfloor\tfrac{i}{3}\right\rfloor\sin\left(\theta_2-\theta_3\right)\left[\frac{d_1}{L_1^G}\sin\left(\theta_1-\theta_2\right)\cos\left(\theta_0-\theta_1\right)\right]\right\}\omega\\
\dot{v} &= \sigma_1 := F/m,\\
\dot{\omega} &= \sigma_2 := \Gamma/I,
\end{aligned}\right\} \quad (1)
$$

In thisresearch, given the *clearance parameters* ε_1 and ε_2 the authors enclose the articulated vehiclewithin separate protective circular regions (as seen inFig. 2), i.e. a protective region for each solidbody, which basically reduces the unnecessary growth of theC-space inas [8] and subsequently presents a greaterset of options. Hence, circular region C_i is centered at (x_i, y_i) for $i = 0,...,3$, with radius

$$r_{V0} = \tfrac{1}{2}\left[\left(L_0+2\varepsilon_1\right)^2+\left(l+2\varepsilon_2\right)^2\right]^{\frac{1}{2}} = \tfrac{L_0+2d_0}{2} \text{ and}$$

$$r_{Vi} = \tfrac{1}{2}\left[\left(L_i^G-a\right)^2+\left(l+2\varepsilon_2\right)^2\right]^{\frac{1}{2}} = \tfrac{L_i^G+d_i}{2}.$$

If we let $L_i^G = L_0 + d_0$ for $i = 1,...,3$ then $r_{V0} = r_{Vi}$. Also with the choice of the reference points and theradius of the circular regions of the vehicles, we have $d_0 = d_i$ for $i = 1,...,3$.

III. Attractive Potential Field functions

This section formulates collision free trajectories of the robot system under kinodynamic constraints in a fixed and bounded workspace. It is assumed that the car-like robots have *priori* knowledge of the whole workspace. We want to design the acceleration controllers, σ_1 and σ_2, so that the mobile robot moves safely towards itstarget.

A. Attraction to Target

A target is assigned for the robot to reach after some time *t*. For the *i*th body of the tractor trailer system, we define a target

$$T = \left\{(z_1,z_2)\in\mathbb{R}^2 : (z_1-p_{i1})^2+(z_2-p_{i2})^2 \le rt_i^2\right\}$$

with center (p_{i1}, p_{i2}) and radius rt_i. For the attraction to its designated target, we consider an attractive potential function

$$V(\mathbf{x}) = \tfrac{1}{2}\left\{\sum_{i=0}^{3}\left[(x_i-p_{i1})^2+(y_i-p_{i2})^2\right]+v^2+\omega^2\right\} \quad (2)$$

B. Auxiliary Function

To guarantee the convergence of the mobile robot to its designated target, we design an auxiliary function defined as:

$$G(\mathbf{x}) = \tfrac{1}{2}\sum_{i=0}^{3}\left[(x_i-p_{i1})^2+(y_i-p_{i2})^2+\rho_i(\theta_i-p_{i3})^2\right] \quad (3)$$

where p_{i3} is the desired final orientation of the *i*th body of the articulated robot. These potential functionsare then multiplied to the repulsive potential functions to be designed in the following sections.

IV. Repulsive Potential Field Functions

We desire the *i*th body of the mobile robot to avoid all stationary obstacles intersecting their paths. For this, we construct the obstacle avoidance functions that merely measure the distances between each body and the obstacles in the workspace. To obtain the desired avoidance, these potential functions appear in the denominator of the repulsive potential field functions. This creates a repulsive field around the obstacles.

A. Fixed Obstacles in the Workspace

Let us fix *w* solid obstacles within the workspace and assume that the *q*th obstacle is circular with center (o_{q1}, o_{q2}) and radius ro_q. For the *i*thbody with a circular avoidance region of radius r_{Vi} to avoid the *l*th obstacle, we adopt

$$FO_{iq}(\mathbf{x}) = \frac{1}{2}\left[(x_i-o_{q1})^2+(y_i-o_{q2})^2-(ro_q+r_{Vi})^2\right] \quad (4)$$

for $i = 0,...,3$ and $q = 0,...,w$.

B. Workspace Limitations

We desire to setup a framework for the workspace of our robot. Our workspace is a fixed, closed and boundedrectangular region, defined, for some $\eta_k > 2r$ for *k*=1, 2 with

$$r = \sum_{i=0}^{3} r_{Vi} \text{ as } WS = \left\{(z_1,z_2)\in\mathbb{R}^2 : 0\le z_1\le\eta_1, 0\le z_2\le\eta_2\right\}.$$

We require the robot to stay within the rectangular region at alltime $t \geq 0$. Therefore, we impose the following boundaryconditions:

Left Boundary: $(z_1, z_2): z_1 = 0$,

Upper Boundary: $(z_1, z_2): z_2 = \eta_2$,

Right Boundary: $(z_1, z_2): z_1 = \eta_1$,

Lower Boundary: $(z_1, z_2): z_2 = 0$.

In our Lyapunov-based control scheme, these boundaries areconsidered as *fixed obstacles*. For the *i*th body of each robot to avoid these, we define the following potential functions for the left, upper, right and lower boundaries, respectively:

$$W_{i1} = x_i - r_{Vi}, \tag{5}$$

$$W_{i2} = \eta_2 - (y_i + r_{Vi}), \tag{6}$$

$$W_{i3} = \eta_1 - (x_i + r_{Vi}), \tag{7}$$

$$W_{i4} = y_i - r_{Vi} \tag{8}$$

for $i = 0,...,3$. Now, since $\eta_k > 2\left(\sum_{i=0}^{3} r_{Vi}\right)$ for $k = 1, 2$ each of the functions is positive in *WS*.Embedding these functions into the control laws will contain themotions of the tractor-trailer robot within the specifiedboundaries of the workspace and will prevent it from crossing overthe boundaries.

C. Orientations

One difficulty that exists with continuous time-invariantcontrollers is that although the final position is reachable, itis virtually impossible to get exact orientations at the equilibrium point of this special class of dynamical systems, adirect result of Brockett's Theorem [9].

In this paper, we construct ghost walls along the sides of thetarget parallel to the desired final orientation of the robot, anda third ghost wall erected in-front of the target. This techniquereduces the possible entry routes to a single opening as the otherentry routes are blocked by the ghost walls.Next, we utilize an idea inspired by the work carried out byKhatib in [1], for the avoidance of these ghost wallsin order to force the desired orientations. The technique we usecalculates the minimum distance from the robot to a ghost wall andavoids the resultant point on that ghost wall. Avoiding theclosest point on any line basically affirms that the mobile robotavoids the whole wall. This algorithm helps greatly simplify thenavigation laws.

Now let us consider the *k*th ghost wall in the (z_1, z_2)-plane, from the point (a_{k2}, b_{k2}) to the point (a_{k1}, b_{k1}). We assume that the point (x_i, y_i) isclosest to it at the tangent line which passes through the point.From geometry, it is known that if (Lx_{ik}, Ly_{ik}) is thepoint of intersection of this tangent, then

$$Lx_{ik} = a_{k1} + \lambda_{ik}(a_{k2} - a_{k1}) \ , Ly_{ik} = b_{k1} + \lambda_{ik}(b_{k2} - b_{k1})$$

where $\lambda_{ik} = (x_i - a_{k1})d_k + (y_i - b_{k1})r_k$, and $d_k = \frac{(a_{k2} - a_{k1})}{(a_{k2} - a_{k1})^2 + (b_{k2} - b_{k1})^2}$, $r_k = \frac{(b_{k2} - b_{k1})}{(a_{k2} - a_{k1})^2 + (b_{k2} - b_{k1})^2}$ If $\lambda_{ik} \geq 1$ then we let $\lambda_{ik} = 1$, if $\lambda_{ik} \leq 0$, then we let $\lambda_{ik} = 0$, otherwise we accept the value of λ_{ik} between 0 and 1, in which case there is a perpendicular line to the point (Lx_{ik}, Ly_{ik}) on the ghost wall from the center (x_i, y_i) of *i*th body of the articulated vehicle at every time $t \geq 0$ .For the *i*th body of the robot to avoid the closest point of eachof the *k*th line segment, we consider a positive potential fieldfunction:

$$LS_{ik}(\mathbf{x}) = \frac{1}{2}\left[(x_i - Lx_{ik})^2 + (y_i - Ly_{ik})^2 - r_{Vi}^{\ 2}\right] \tag{9}$$

for $i = 0,...,3$ and $k = 1,...,m$.

V. Dynamic Constraints

Practically, the steering and bending angles of themobile robots are limited due to mechanical singularities while the translational speed is restricted due to safety reasons. Subsequently, we have; $(\mathbf{i})$ $|v| \leq v_{max}$, where v_{max} is the maximal speed of the tractor; $(\mathbf{ii})$ $|\phi| \leq \phi_{max} < \frac{\pi}{2}$, where ϕ_{max} is the maximal steering angle, and $(\mathbf{iii})$ $|\theta_i - \theta_{i-1}| \leq \theta_{\max} < \frac{\pi}{2}$ where $\theta_{\max}$ is the *maximum bending angle* of the trailer with respect to the orientation of the tractor. The trailer can freely rotate within $(-\frac{\pi}{2}, \frac{\pi}{2})$ about their linking point with the tractor.

Considering these constraints as artificial obstacles, we have the following potential field functions:

$$U_1(\mathbf{x}) = \tfrac{1}{2}\left[(v_{\max} - v)(v_{\max} + v)\right] \tag{10}$$

$$U_2(\mathbf{x}) = \tfrac{1}{2}\left[\left(\frac{v_{\max}}{|\rho_{\min}|} - \omega\right)\left(\frac{v_{\max}}{|\rho_{\min}|} + \omega\right)\right] \tag{11}$$

$$DC_i(\mathbf{x}) = \tfrac{1}{2}\left[(\theta_{\max} - (\theta_i - \theta_{i-1}))(\theta_{\max} + (\theta_i - \theta_{i-1}))\right] \tag{12}$$

These potential functions guarantee the adherence to the above restrictions placed upon the translational velocity v, steering angle ϕ, and the rotation θ_i, for the *i*th trailer.

VI. Control Laws

Combining all the potential functions $(2-12)$, and introducing constants, denoted as the control parameters, $\alpha_{ik}, \beta_{ij}, \zeta_j, \gamma_{iq}, \kappa_s > 0$ $i, j, k, q, s \in \mathbb{N}$, we define a candidate Lyapunov function

$$L(\mathbf{x}) = V(\mathbf{x}) + G(\mathbf{x})\sum_{i=0}^{3}\left[\sum_{k=1}^{2}\frac{\alpha_{ik}}{LS_{ik}(\mathbf{x})} + \sum_{j=1}^{4}\frac{\beta_{ij}}{W_{ij}(\mathbf{x})}\right] + G(\mathbf{x})\left[\sum_{j=1}^{3}\frac{\zeta_j}{DC_j(\mathbf{x})} + \sum_{q=1}^{w}\frac{\gamma_{iq}}{FO_{iq}(\mathbf{x})} + \sum_{s=1}^{2}\frac{\kappa_s}{U_s(\mathbf{x})}\right] \quad (10)$$

Clearly, $L(\mathbf{x})$ is locally positive and continuous on the domain $D(L) = \{\mathbf{x} \in \mathbb{R}^8 : W_{ij}(\mathbf{x}) > 0,\ LS_{ik}(\mathbf{x}) > 0,\ FO_{iq}(\mathbf{x}) > 0,\ DC_j(\mathbf{x}) > 0, U_s(\mathbf{x}) > 0\}$. We define $\mathbf{x}_e := (p_{i1}, p_{i2}, p_{i3}, 0, 0)$ an equilibrium point of system(1). Thus, we have $L(\mathbf{x}_e) = 0$.

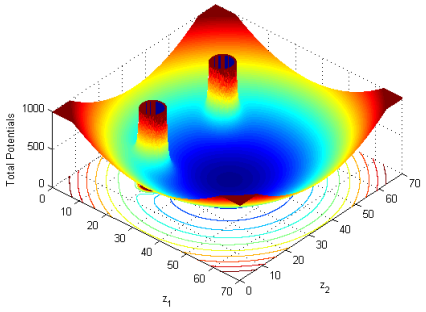

Fig. 3 The total potential

The total potentials as in Fig. 3 aregenerated for target attraction and avoidance of two stationary disk-shaped obstacles. For better visualization the target of the leader is located at $(t_1, t_2) = (35, 35)$, and the disks are fixed at $(o_{11}, o_{12}) = (9, 10)$, $(o_{21}, o_{22}) = (11, 19)$ with radii of $ro_1 = ro_2 = 1.2$, while $\alpha_{1l} = 20$, $l = 1, 2$. Also, the velocity and angular components of the robot have been treated as constants such that $v = 0.5$, $\omega = 0$, and $\theta_0 = 0$.

To extract the control laws, we differentiate the various components of $L(\mathbf{x})$ separately and carry out the necessary substitutions from (1). The nonlinear control laws for system (1) will be designed using Lyapunov's Direct Method. The process begins with the following theorem:

Theorem: *The equilibrium point* $\mathbf{x}_e$ *of system(1) is stable in the sense of Lyapunov provided*

$$\sigma_1 = -\frac{1}{d_1(\mathbf{x})}\left[\delta_1 v + \sum_{i=0}^{n}\left(f_i(\mathbf{x})\cos\theta_0 + g_i(\mathbf{x})\sin\theta_0\right) + \sum_{i=1}^{n-1}\frac{1}{L_i^G}m_{i+1}(\mathbf{x})\dot{u}_i\right] - \frac{1}{d_1(\mathbf{x})}\left\{\sum_{i=1}^{n}\left[\left(\frac{L_i^G + d_i}{2L_i^G}\right)f_i(\mathbf{x})\sin\theta_i + h_i(\mathbf{x}) - m_i(\mathbf{x})\right]\dot{u}_i\right\} - \frac{1}{d_1(\mathbf{x})}\left\{\sum_{i=1}^{n}\sum_{j=1}^{i-1}\left(\frac{L_j^G + d_j}{L_i^G}\right)\left[f_i(\mathbf{x})\sin\theta_j - g_i(\mathbf{x})\cos\theta_j\right]\dot{u}_i\right\} \quad (13)$$

and

$$\sigma_2 = -\frac{1}{d_2(\mathbf{x})}\left[\delta_2\omega + \frac{L_0}{2}\left(g_0(\mathbf{x})\cos\theta_0 - f_0(\mathbf{x})\sin\theta_0\right) + \sum_{i=1}^{n-1}\frac{d_1}{L_i^G}m_{i+1}(\mathbf{x})\dot{z}_i\right] - \frac{1}{d_2(\mathbf{x})}\left[d_1\left\{\sum_{i=1}^{n}\sum_{j=1}^{i-1}\left(\frac{L_j^G + d_j}{L_i^G}\right)\left[f_i(\mathbf{x})\sin\theta_j - g_i(\mathbf{x})\cos\theta_j\right]\dot{z}_i + h_0(\mathbf{x})\right\}\right] - \frac{1}{d_2(\mathbf{x})}\left[d_1\sum_{i=1}^{n}\left[\left(\frac{L_i^G + d_i}{2L_i^G}\right)f_i(\mathbf{x})\sin\theta_i - h_i(\mathbf{x}) - m_i(\mathbf{x})\right]\dot{z}_i + m_1(\mathbf{x})\right] \quad (14)$$

for $i = 1, \ldots, n$, *where* $\delta_1, \delta_2 > 0$ *are constants commonly known as convergence parameters and* $n = 3$.

Proof: The time derivative of our Lyapunov function $L(\mathbf{x})$ along a particular trajectory of system (1) is then:

$$\dot{L}_{(1)}(\mathbf{x}) = -\sum_{i=1}^{n}\left(\delta_1 v^2 + \delta_2\omega^2\right) \le 0 \text{ for all } \mathbf{x} \in D(L), \text{ and } \dot{L}_{(1)}(\mathbf{x}_e) = 0$$

where the functions $f_i, g_i, h_i, g_i, m_j, d_s$ for $i, j = 1, \ldots, 3$, $n = 3$ and $s = 1, 2$ are defined as (upon suppressing $\mathbf{x}$):

$$f_i = \left[1 + L_i(\mathbf{x})\right](x_i - p_{i1}) - G(\mathbf{x})\left[\frac{\beta_{i1}}{W_{i1}^2(\mathbf{x})} - \frac{\beta_{i3}}{W_{i3}^2(\mathbf{x})}\right] - G(\mathbf{x})\sum_{q=1}^{w}\frac{\gamma_{iq}}{FO_{iq}^2(\mathbf{x})}(x_i - o_{q1}) - G(\mathbf{x})\sum_{k=1}^{2}\frac{\alpha_{ik}}{LS_{ik}^2(\mathbf{x})}(1 - (a_{k2} - a_{k1}))d_k(x_i - Lx_{ik}) + G(\mathbf{x})\sum_{k=1}^{2}\frac{\alpha_{ik}}{LS_{ik}^2(\mathbf{x})}(b_{k2} - b_{k1})d_k(y_i - Ly_{ik}),$$

$$h_i = L_i(\mathbf{x})(\theta_i - p_{i3}),$$

$$g_i = \left[1 + L_i(\mathbf{x})\right](y_i - p_{i2}) - G(\mathbf{x})\left[\frac{\beta_{i4}}{W_{i4}^2(\mathbf{x})} - \frac{\beta_{i2}}{W_{i2}^2(\mathbf{x})}\right] - G(\mathbf{x})\sum_{q=1}^{w}\frac{\gamma_{iq}}{FO_{iq}^2(\mathbf{x})}(y_i - o_{q2}) - G(\mathbf{x})\sum_{k=1}^{2}\frac{\alpha_{ik}}{LS_{ik}^2(\mathbf{x})}(1 - (b_{k2} - b_{k1}))r_k(y_i - Ly_{ik}) + G(\mathbf{x})\sum_{k=1}^{2}\frac{\alpha_{ik}}{LS_{ik}^2(\mathbf{x})}(a_{k2} - a_{k1})r_k(x_i - Lx_{ik}),$$

$$m_j = G(\mathbf{x})\frac{\zeta_s}{DC_j^2(\mathbf{x})}(\theta_j - \theta_{j-1}),$$

$$d_s = 1 + G(\mathbf{x})\frac{\kappa_s}{U_s^2(\mathbf{x})},$$

where

$$L_i(\mathbf{x}) = \sum_{k=1}^{2}\frac{\alpha_{ik}}{LS_{ik}(\mathbf{x})} + \sum_{j=1}^{4}\frac{\beta_{ij}}{W_{ij}(\mathbf{x})} + \sum_{j=1}^{3}\frac{\zeta_j}{DC_j(\mathbf{x})} + \sum_{q=1}^{w}\frac{\gamma_{iq}}{FO_{iq}(\mathbf{x})} + \sum_{s=1}^{2}\frac{\kappa_s}{U_s(\mathbf{x})},$$

and

$$\dot{u}_i = \Bigg\{ \sin(\theta_{i-1}-\theta_i)\left[\prod_{j=1}^{i-1}\cos(\theta_{j-1}-\theta_j)\right] + \left\lfloor \tfrac{i}{2} \right\rfloor (-1)^{i+1}\sin(\theta_0-\theta_1)\left[\prod_{j=2}^{i}\frac{d_{j-1}}{L_{j-1}^G}\cos(\theta_{j-1}-\theta_j)\right] + \left\lfloor \tfrac{i}{3} \right\rfloor \sin(\theta_1-\theta_2)\left[\frac{d_1}{L_1^G}\sin(\theta_2-\theta_3)\sin(\theta_0-\theta_1)\right] - \left\lfloor \tfrac{i}{3} \right\rfloor \sin(\theta_1-\theta_2)\left[\frac{d_2}{L_2^G}\cos(\theta_2-\theta_3)\cos(\theta_0-\theta_1)\right] \Bigg\},$$

$$\dot{z}_i = \Bigg\{ (-1)^i\cos(\theta_0-\theta_1)\left[\prod_{j=1}^{i-1}\frac{d_j}{L_j^G}\cos(\theta_j-\theta_{j+1})\right] + \left\lfloor \tfrac{i}{2} \right\rfloor (-1)^i\left[\prod_{j=0}^{1}\sin(\theta_j-\theta_{j+1})\right]\left[\prod_{k=3}^{i}\frac{d_{k-1}}{L_{k-1}^G}\cos(\theta_{k-1}-\theta_k)\right] + \left\lfloor \tfrac{i}{3} \right\rfloor \sin(\theta_2-\theta_3)\left[\cos(\theta_1-\theta_2)\sin(\theta_0-\theta_1)\right] - \left\lfloor \tfrac{i}{3} \right\rfloor \sin(\theta_2-\theta_3)\left[\frac{d_1}{L_1^G}\sin(\theta_1-\theta_2)\cos(\theta_0-\theta_1)\right] \Bigg\}.$$

A careful scrutiny of the properties of our scalar function reveals that $\mathbf{x}_e$ is an equilibrium point of system (1) in the sense of Lyapunov and $L(\mathbf{x})$ is a legitimate Lyapunov function guaranteeing stability. This is in no contradiction with Brockett's result [11] as we have not proven asymptotic stability.

VII. Simulation

To illustrate the effectiveness of the proposed controllers, we present a scenario, see Fig. 4,of where the car-like robot and its passive trailers move towards its designated goal while avoiding fixed obstacles in its workspace. The use of the ghost walls helps in attaining the desired posture of the tractor and the trailer robots.

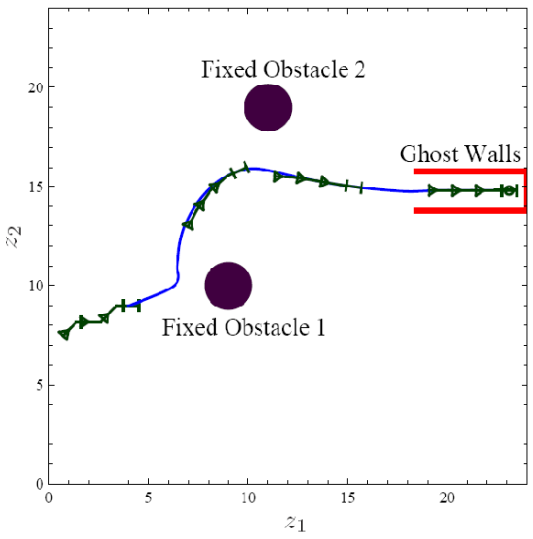

Fig. 4 The resulting stable trajectory of the general 3-trailer robot

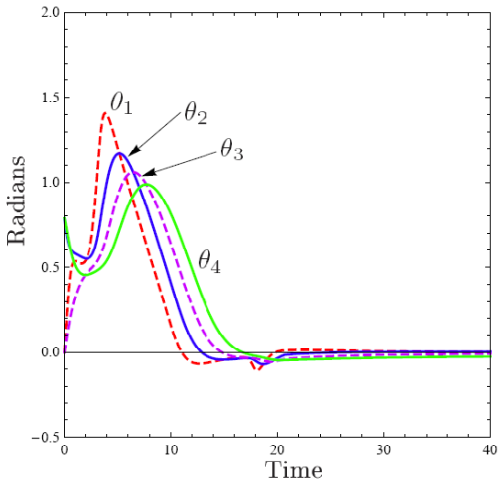

Fig. 5 Orientations of the tractor and its trailers

TABLE I
Numerical Values of Initial States, Constraints and Parameters for Scenario 1

		Initial Conditions
Initial Configuration		$(x_0, y_0) = (5,10)$, $v = 0.5$, $\omega = 0$, $(\theta_0, \theta_2, \theta_3, \theta_4) = (0, \frac{\pi}{4}, 0, \frac{\pi}{4})$
Final Configuration		$(p_{01}, p_{02}, p_{03}, p_{13}, p_{23}, p_{33}) = (23, 14.5, 0, 0, 0, 0)$
Fixed Obstacles		$(o_{11}, o_{12}) = (9,10), (o_{21}, o_{22}) = (11,19)$, $ro_1 = ro_2 = 1.2$
Physical Limitations		$v_{\max} = 5$, $\phi_{\max} = \frac{\pi}{2}$, $\rho_{\min} = 0.14$
Dimensions of Robots		$L_1 = 0.75$, $L_i^G = 0.965$, $l = 0.5$, $c = d_i = 0.215$, $\omega = 1.2$
Workspace Boundaries		$\eta_1 = \eta_2 = 24$
Clearance Parameters		$\varepsilon_1 = \varepsilon_2 = 0.1$
Safety Parameters		$\xi_1 = \xi_2 = 0.41$
Control Parameters	Ghost Walls	$\alpha_{ik} = 0.01$
	Fixed Obstacles	$\gamma_{0q} = 8, \gamma_{1q} = 2, \gamma_{2q} = 3, \gamma_{3q} = 3$
	Dynamic Constraints	$\xi_1 = \xi_2 = 1, \xi_3 = 3, \kappa_s = 1$
	Workspace Restrictions	$\beta_{ij} = 1$
Convergence Parameters		$\delta_1 = \delta_2 = 120$

Graph in Fig. 5 show the orientations of the tractor and its 3 off-axle trailers.The corresponding initial and final states and other details for the simulation are listed in Table I (assuming that appropriate units have been taken into account).

VIII. Conclusion

This paper presents a set of artificial field functions derived using Lyapunov's direct method that improves upon, in general, the posture control with theoretically guaranteed point and posture stabilities, and convergence and collision avoidance of a general 3-trailer mobile robot. We have a

centralized trajectory planning algorithm, which to some extent, demonstrates autonomy and multitasking capabilities of humans. The new algorithm provides us with a suitable and fitting platform to harvest collision-free trajectories from initial to desired states and generate maneuvers that culminate to practically reasonable postures within a constrained environment, whilst satisfying the nonholonomic constraints of the system. The proposed controllers stabilize the configuration coordinates of the vehicle to an arbitrary smallneighborhood of the target. We note here that convergence is only guaranteed from a number of initial states of the system.

The derived controllers produced feasible trajectories and ensured a nice convergence of the system to its equilibrium state while satisfying the necessary kinematic and dynamic constraints. We note here that convergence is only guaranteed from a number of initial states of the system.

Future research will address a swarm of thegeneral 3-trailermobile robots.

REFERENCES

[1] O. Khatib, "Real-time obstacle avoidance for manipulators and mobile robots", *International Journal of Robotics Research* 5 (1): 90–98, March, 1986.

[2] A. W. Divelbiss and J. T. Wen., "Trajectory tracking control of a car-trailer system", *IEEE Transactions on Control Systems Technology*, 5(3):269-278,1997.

[3] P. Bolzern, R.M. DeSantis, and A.Locatelli. "An input-output linearisation approach to the control of an *n* body articulated vehicle", Journal of Dynamic Systems, Measurement, and Control,123(3):309-316, 2001.

[4] J. Lee, W. Chung, M. Kim, C. Lee, and Jeabok-Song, "A passive multipletrailer system for indoor service robots," in *IEEE/RSJ Int. Conf.Intelligent Robots and Systems*, Maui, HI, 2001, pp. 827–832.

[5] Sharma. B, Vanualailai. J, Raghuwaiya. K and Prasad. A, (2008), "New Potential Field Functions for Motion Planning and Posture Control of 1-Trailer Systems", *International Journal of Mathematics and Computing Science*, 3(1): 45-71.

[6] Sharma.B, Vanualailai. J, and Chand. U, (2009) "Flocking of Multi-agents in Constrained Environments", *European Journal of Pure and Applied Mathematics*, 2(3): 401-425.

[7] K. Raghuwaiya, S. Singh, B. Sharma, and J. Vanualailai, "Autonomous Control of a Flock of 1-Trailer Mobile robots", *Procs of the 2010 International Conference on Scientific Computing*, , Las Vegas, USA, 2010, pp 153-158.

[8] K. Raghuwaiya, S. Singh, B. Sharma, G. Lingam, " Formation Types of a Flock of 1-Trailer Mobile Robots," *Procs of The 7th IMT-GT International Conference on Mathematics, Statistics and its Applications*, Bangkok, Thailand, 2011, pp 368-382.

[9] B. Sharma, "*New Directions in the Applications of the Lyapunov-based Control Scheme to the Findpath Problem*", PhD Dissertation, University of the South Pacific, Fiji, July 2008.

[10] P. C-Y. Sheu and Q. Xue, *Intelligent Robotic Planning Systems*, World Scientific, Singapore, 1993.

[11] R. W. Brockett, "*Differential Geometry Control Theory*",chapter Asymptotic Stability and Feedback Stabilisation, pages 181-191. Springer-Verlag, (1983).